Developing an empirical model for added turbulence in a wake of tidal turbine

Kabir Bashir Shariff, Sylvain S. Guillou

▶ **To cite this version:**

Kabir Bashir Shariff, Sylvain S. Guillou. Developing an empirical model for added turbulence in a wake of tidal turbine. 25 ème Congrès Français de Mécanique, Aug 2022, Nantes, France. hal-03768506

HAL Id: hal-03768506

https://normandie-univ.hal.science/hal-03768506v1

Submitted on 3 Sep 2022

HAL is a multi-disciplinary open access archive for the deposit and dissemination of scientific research documents, whether they are published or not. The documents may come from teaching and research institutions in France or abroad, or from public or private research centers.

L'archive ouverte pluridisciplinaire **HAL**, est destinée au dépôt et à la diffusion de documents scientifiques de niveau recherche, publiés ou non, émanant des établissements d'enseignement et de recherche français ou étrangers, des laboratoires publics ou privés.

Developing an empirical model for added turbulence in a wake of tidal turbine

K. SHARIFF* and S. GUILLOU

Normandie Université, UNICAEN, LUSAC, EA4253, 60 rue Max Pol Fouchet, 50130, Cherbourg-Octeville, France
kabir-bashir.shariff@unicaen.fr, sylvain.guillou@unicaen.fr

Keywords : Tidal turbine, actuator disc, added turbulence, empirical model, wake.

Abstract

The increased turbulence behind the turbine induces fatigue loads on the downstream turbine blades. Accurate estimation of turbulent intensity in turbine wake is paramount to optimising the placement of turbines in tidal turbine parks. A simple empirical model is developed using data fitting from a numerical simulation of a non-rotational actuator disc model to estimate the added turbulence in a tidal flow condition similar to the Raz Blanchard site. The empirical model justifies that the major turbulence source in the near wake is attributed to the rotor and the added turbulence is slightly dependent on the ambient turbulence in the flow. As no known available empirical model for the tidal turbine, the model is compared with the IEC 61400 standard for an unbounded wind turbine.

1 Introduction

Tidal stream turbines (TST) harness the kinetic energy of the tides into electrical energy. The energy extraction process attenuates the kinetic energy of the tide in form of the wake. Wake is a region of disturbed flow behind the turbine. The two main characteristics of wake are the significant velocity deficit that reduces the power extracted by the turbine downstream and increased turbulence that induced fatigue loading on the turbine (Quarton & Ainslie, 1990; Chamorro & Porté-Agel, 2009).

The limited availability of field measurement and huge computational cost at full scale inspire the development of a simple analytical model to investigate the wake behind the turbine. These investigations mainly focused on the velocity deficit as it directly affects the power extracted by the turbine ($P \propto U^3$). Few empirical relations were developed to estimate the added turbulence of wind turbines. The added turbulence relation reported is expressed as a function of the flow condition and turbine characteristics (Quarton & Ainslie, 1990; Crespo, Herna, et al., 1996; Frandsen & Thøgersen, 1999). These models provide a single value of the added turbulence at the center line. In contrast to wind turbines, tidal turbines are usually located in shallow water constrained by the channel depth. The use of a wind turbine model may result in improper estimation.

Accurate knowledge of wake turbulence is important primarily because it enables the evaluation of additional fatigue loading on turbine blades and ensures a proper location for turbine placement downstream (Frandsen & Thøgersen, 1999; Mullings & Stallard, 2021). To the best of our knowledge, there is no

simple empirical model to estimate the turbulent intensity in the wake of a tidal turbine. To this effect, this study aims to develop a simple empirical model to estimate the turbulent intensity in the wake of a rotor in realistic tidal stream conditions.

2 Turbulence in turbine wake

Turbulent intensity is defined as a ratio of standard deviation (σ) or the root mean square (u_{rms}) or turbulent velocity fluctuation ($u^{'}$) to the mean velocity expressed as Eq. (1):

$$\mathrm{I} = \frac{\sigma_{\mathrm{u}}}{\mathrm{U}} = \frac{\mathrm{u_{rms}\ or\ u'}}{\mathrm{U}} \tag{1}$$

The total turbulent intensity in the wake is expressed in terms of ambient turbulence in the flow and added turbulence generated by the turbine (Quarton & Ainslie, 1990):

$$\mathrm{I_{wake}} = \left(\mathrm{I_a^2} + \mathrm{I_+^2}\right)^{0.5} \tag{2}$$

where I_{wake} is the total turbulence in the wake, I_a is the ambient turbulence and I_+ is the added turbulence by the rotor. The added turbulence is the additional turbulent kinetic energy induced by the turbine and the shear layer developed at the tip of the blade. A schematic diagram of tidal turbine wake is shown in Figure 1.

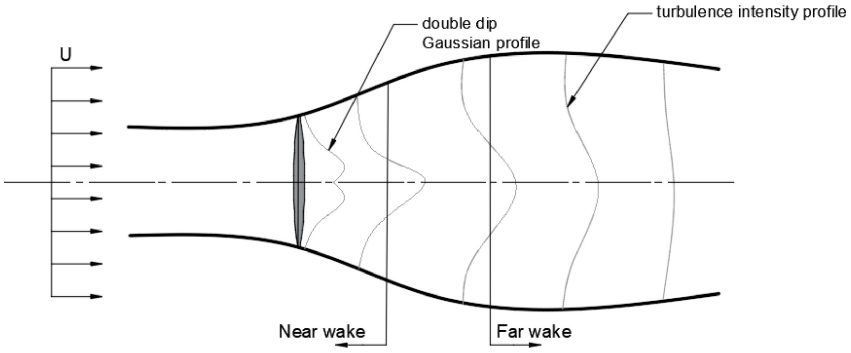

Figure 1: Schematic of the wake behind tidal turbine showing the evolution of turbulent intensity downstream along the lateral plane.

The wake behind a turbine is broadly categorized into two regions; near wake and far wake region Vermeer et al., (2003). The intensity of turbulence varies depending on the location. The near wake region (< 4 D downstream) is attributed to the highest turbulence due to the additional contribution of the shear and turbine generated turbulence, while the far wake region (>7 D downstream) is mainly influenced by the ambient turbulence in the flow.

3 Numerical method and case set-up

A 3D steady-state numerical simulation is performed with open-source code *OpenFOAM*. Several CFD simulations of tidal turbines used steady Reynolds-Average Navier Stokes (RANS) turbulence models considering only statistically time-averaged mean flow (Harrison et al., (2010); Nguyen et al., (2016);

Jump et al., (2020)). Although in reality, a significant fluctuation occurs with eddies structure in a streamwise direction roughly as large as the turbine diameter (Gant & Stallard, 2008) , the changes in mean performance are similar to a steady flow condition (Zhang et al., 2020). The turbine is represented as a porous disc using the actuator disc method (ADM). ADM has been widely used by several authors (Harrision et al., (2010); Nguyen et al., (2016)) and has proven to provide a relatively good result for tidal turbine applications in comparison with experimental studies in the far wake region (Abolghasemi et al., 2016). In the ADM, a uniform thrust force is applied to the rotor to create a pressure jump and momentum exchange similar to a real turbine. Thrust force applied on disc region is calculated as Eq. (3):

$$T = \frac{1}{2}\rho C_T S U_\infty^2 \tag{3}$$

where ρ is the fluid density, S is the rotor cross-sectional area, U_∞ is the upstream velocity and C_T is the thrust coefficient. In the case of multiple turbines, the definition by the upstream velocity becomes questionable, therefore a modification is required to define the thrust force in terms of local velocity at the disc location. A resistance coefficient, K which relates to C_T is proposed by Taylor (1958) to calculate the thrust force at the disc location as:

$$C_T = \frac{K}{\left(1 + \frac{1}{4}K\right)^2}, \qquad T = \frac{1}{2}\rho\frac{K}{e}U_d^2, \tag{4}$$

where U_d is the velocity at the disc and K is the resistance coefficient and e is the disc thickness.

The thrust force is added as a volumic source (here as a sink for extraction of energy) to the momentum equation and solved along with the continuity equation.

A standard $k-\epsilon$ turbulence model is used for turbulence closure of Reynold stress. Although the $\kappa-\epsilon$ model is shown to provide good results in far wake compared to the porous disc experiments (Nguyen et al., 2016). It tends to predict faster wake recovery due to the failure to account for energy cascade from large scale to small scale in the near wake region (Roc et al., (2013)). Therefore, the use of turbulence correction to compliment the added turbulence generated by the turbine is suggested (Shives & Crawford, 2016).

3.1 Model validation

A validation study of 3 bladed tidal turbine experiment study by Mycek et al., (2014) is carried out with a 0.7m diameter rotor. The turbulent intensity in the channel is 15%, upstream velocity in the channel is 0.83 m/s. The thrust and power coefficient recorded is C_T = 0.75 and C_P = 0.38 respectively.

To account for the proper turbulence cascading in the near wake, turbulence correction with source term added to the turbulence model has been proposed for wind turbines by Réthoré et al.,(2009). The source term parameters have been tuned for with tidal turbine experimental data of Mycek et al., (Mycek et al., 2014) by Olson et al., (2021). The correction parameters reported by Olson et al., (2021) is used in this validation.

Figure 2 shows the numerical model is in agreement with the experimental data, especially in the far wake. The source term compensates for the turbulent intensity in the near wake. The experimental results are not truly axis symmetry as reported by Mycek et al., (2014), this effect cannot be captured by the actuator disc model because (a) the thrust is uniformly applied on the disc, (b) there is no turbine tower presentation in the actuator disc model and (c) the swirling effect due to turbine rotation (Grondeau et al., 2022). This validates the numerical model, thus providing the basis for the full-scale TST model.

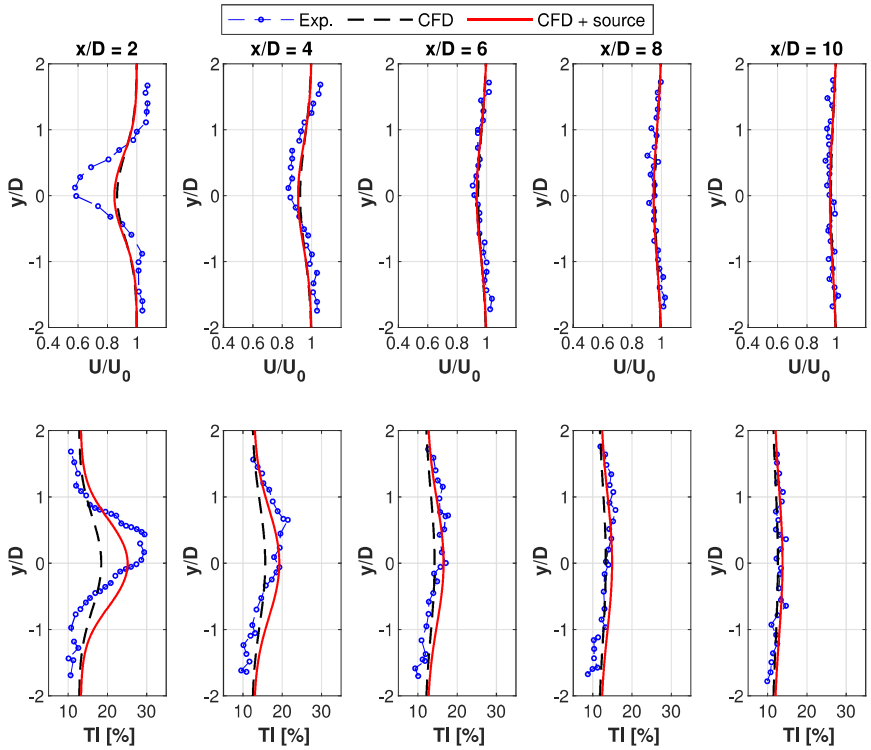

Figure 2: Comparison of a numerical model with TST experimental results (Mycek et al., 2014) at 15% ambient turbulence showing the normalised lateral velocity (top) and the turbulent intensity along the turbine axis (bottom).

3.2 Tidal turbine with realistic dimension

The size of commercial-scale tidal turbines has been increasing recently with turbines ranging from 14 m to 20 m in diameter (Rajgor, 2016). Normandie hydroliennes project is currently in the process of developing and installing a 12 MW pilot tidal farm in the Raz Blanchard. In this study, a 20 m diameter turbine (the size for Atlantis AR2000 (Goss & Coles, 2020)) represented as a disc is located at 10 D (D is the turbine diameter) from the inlet of the domain at mid-depth 2.5 D (c.f 3). The length of the domain is 50 D and the width is 20 D. The channel depth is 50 m similar to the Raz Blanchard (Nguyen et al., (2019)). The blockage ratio in the channel is 1.57%. The blockage ratio is defined as the ratio of the actuator disc to the total cross-sectional area of the domain.

The numerical domain is discretised by structured grid cells with refinement close to the turbine. Grid sensitivity was carried out at different mesh densities and Cells Per Diameter (CPD). 25 CPD across the disc surface for the Δy (transverse) and Δz (depthwise) provide a good disc representation and imperceptible results. The CPD along the Δx (streamwise) direction representing the thickness of the disc is 5. The region far away from the disc is represented by a coarse mesh with a geometric growth rate of 1.2.

A realistic boundary condition of a typical tidal stream is used for the numerical model. A logarithmic velocity and a constant κ and ϵ at the inlet. A no-slip condition is set at the bottom wall with wall functions, and the top and the lateral wall are set to symmetry condition. The outlet of the domain is set to pressure outlet condition corresponding to atmospheric pressure. The inlet condition is expressed as

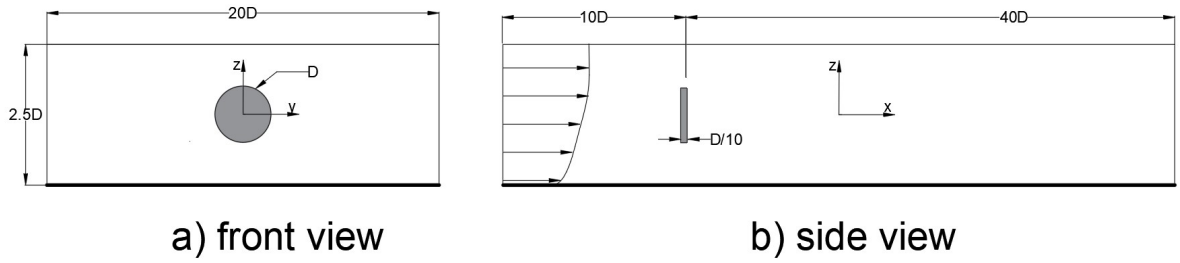

Figure 3: Computational domain showing the channel configuration.

Eq. (5):

$$U = \frac{U^*}{\kappa} \ln\left(\frac{z}{z_0}\right), \qquad k = \frac{3}{2} I^2 U^2, \qquad \epsilon = C_\mu^{\frac{3}{4}} \frac{k^{\frac{3}{2}}}{L} \tag{5}$$

Where U^* = 0.1109 m/s is the frictional velocity, U = 2.7 m/s is mean velocity similar to flow in Raz Blanchard (Thiébaut et al., 2020), κ = 0.4 is von Karman constant, z is the channel depth, z_0 is the roughness and $L = H/3$ is the turbulent length scale, I is the turbulent intensity and C_μ is the turbulence model constant.

In this study, the ambient turbulent intensity I of 5% to 20% is considered to have a global representation of the flow conditions similar to a realistic channel (Mycek et al., 2014). The thrust coefficient of Betz limit corresponding to C_T = 0.89 $(K = 2)$ is used. It is important to clarify that experimental data are not available at this scale of the tidal turbine to fine-tune the turbulence source term parameters to account for the turbine effect, therefore a standard $\kappa - \epsilon$ is used.

However, for empirical models, a definitive value of turbulent intensity upstream of the turbine is essential which can be uncertain in simulation due to turbulence dissipation downstream, especially at high turbulent intensity. Therefore the inlet turbulence condition is maintained in the upstream region. This ensures stable turbulence upstream. This is analogous to the turbulence source term used for wind turbines by El Kasmi & Masson (2008).

4 Results and discussion

4.1 Turbulent wake analysis

Turbulent intensity contour of turbine wake at different ambient turbulence is shown in Figure 4. The maximum turbulent intensity in the wake occurs in the initial near wake. The initial wake is the region behind the turbine where the ambient pressure drop due to momentum extraction is largely recovered. Crespo et al., (1996) define this length to 1-2 D for a wind turbine. This is also consistent with our numerical data as shown in Figure 4. The major contributor to turbulence in this region is the rotor and mean shear.

In the far wake, the turbine effect and the mean shear is weak compared to the near wake. The approximately Gaussian profile is preserved for low turbulence case (I_{amb} = 5%) but vanishes in high turbulent cases (c.f Fig. 4). The turbulent effects vanish rapidly at high turbulence due to strong mixing. The turbulent intensity along the rotor axis and the lateral wall is imperceptible, therefore recognizing the dominance of ambient turbulence in the far wake region. High turbulence produces large turbulent

scales that cascade and diminishes faster than small eddies. Flow recovery has also been reported in experiments to be faster at high ambient turbulence (Mycek et al., 2014).

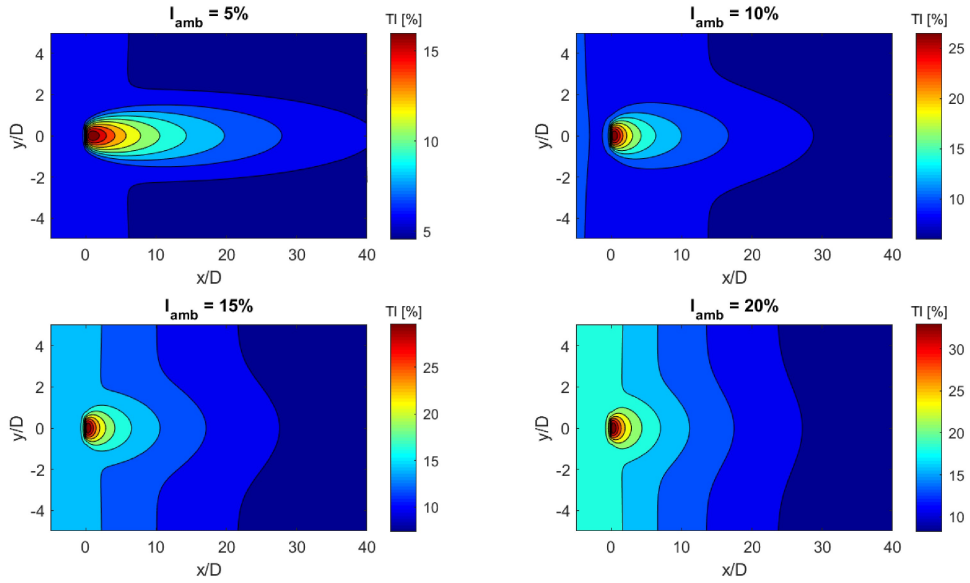

Figure 4: Turbulent intensity contour plot at different ambient conditions showing the effect of added turbulence by the rotor in the near wake region.

4.2 Estimation of centre-line added turbulence

The centerline turbulence is the total turbulence in the wake as expressed in Eq. (2). Added turbulence in the wake is extracted by subtracting the root sum squared of wake turbulence at the centerline and the ambient turbulence close to the lateral wall. The turbulent intensity close to the lateral surface is assumed at the ambient state as it is far away from the rotor as shown in Figure 5.

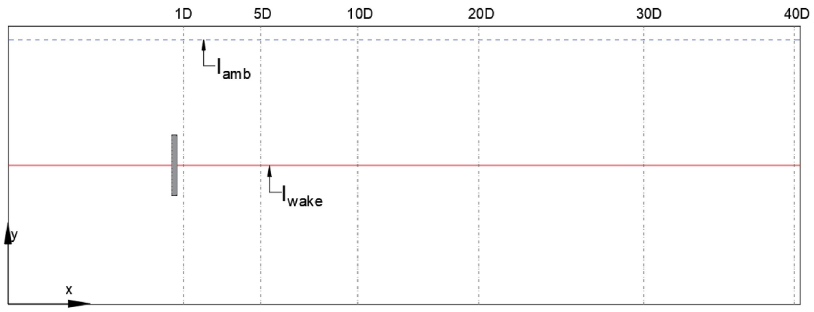

Figure 5: Lateral plane showing the position of ambient and total wake turbulence in the channel.

Assuming the ambient turbulence is stable in the flow. It is sufficient to propose a model for the added turbulence to estimate the turbulence in the wake. As mentioned earlier, the inlet turbulent condition is maintained upstream of the turbine to preclude the dissipation due to the numerical model as shown in Figure 6a. The added turbulence in Fig. 6b shows a slight dependence of the ambient turbulence in the flow. Added turbulence decays downstream as a result of the mixing and diffusion process in the wake. The diffusion at high ambient turbulence is accelerated leading to faster flow recovery (c.f 6a).

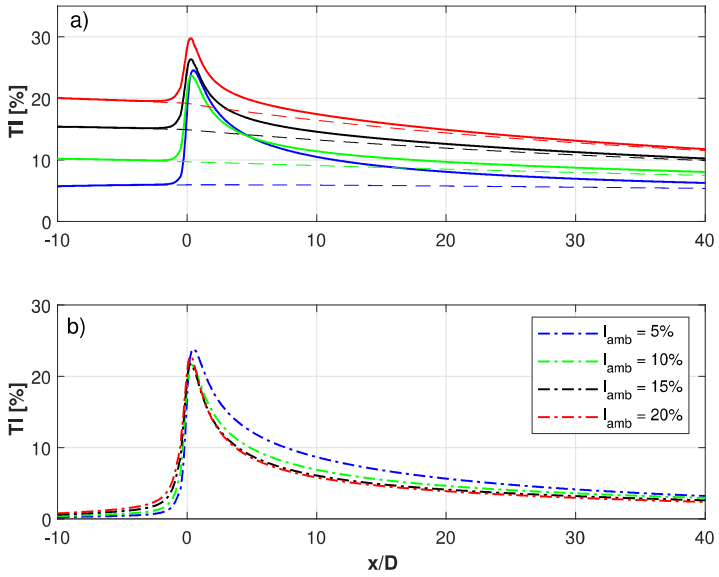

Figure 6: Centreline turbine wake turbulence at different ambient turbulent intensities (a) showing the total turbulence (solid) and ambient turbulence (dash); (b) showing the added turbulence (dash-dot).

4.3 Added turbulent intensity model

The previous models of added turbulence in the wake of a wind turbine are expressed as a function of turbine and flow characteristics (Crespo et al., 1996; Frandsen & Thøgersen, 1999). Using our numerical data, a simple model is developed by to estimate the added turbulence in the wake of a tidal turbine using curve fitting in MATLAB. The centerline turbulent intensity profile in Fig. 6b shows a decay in added turbulent intensity downstream. The new centreline added turbulent intensity model is expressed as Eq. (6):

$$I_+ = a(x/D)^{-b} \qquad \begin{cases} a = 0.16C_T^{4.83} + 0.179 \\ b = 0.68I_a + 0.472 \end{cases} \tag{6}$$

The added turbulence due to the rotor is slightly dependent on ambient turbulent intensity as shown in Fig. 6b. This is compatible with the work of Frandsen & Thøgersen (1999) that expressed the added turbulence dependence on thrust coefficient and the position downstream (Eq. (7)). The Frandsen model is adopted by the IEC standard 61400 (IEC, 2019) standards for wind turbine application. Figure 7 shows the numerical data provides a good fit for the proposed model.

$$I_+ = \frac{1}{1.5 + 0.8\frac{x/D}{\sqrt{C_T}}} \tag{7}$$

The attenuation of the kinetic energy of the flow by the rotor generates additional turbulence close to the turbine. As mentioned earlier, the near wake region is dominated by the turbine and shear layer generated turbulence. Our empirical models justify that the major turbulence source in the near wake is attributed to the rotor. A measure of accuracy between the empirical and numerical models is shown in Table 1. The Mean Absolute Percentage Error (MAPE) is calculated as Eq. (8):

$$\text{MAPE} = \frac{1}{N}\sum_{i=1}^{N}\left|\frac{A_i - M_i}{A_i}\right| \cdot 100\% \tag{8}$$

where A_i is the numerical added turbulent intensity and M_i is the empirical model for the added turbulence at 1 D interval downstream. The large error between the two models can be attributed to the different wake structures. The wind turbine wake is axis-symmetric (Qian & Ishihara, 2021) while the tidal turbine wake is largely Gaussian due to the vertically constrained channel depth Stallard et al., (2015).

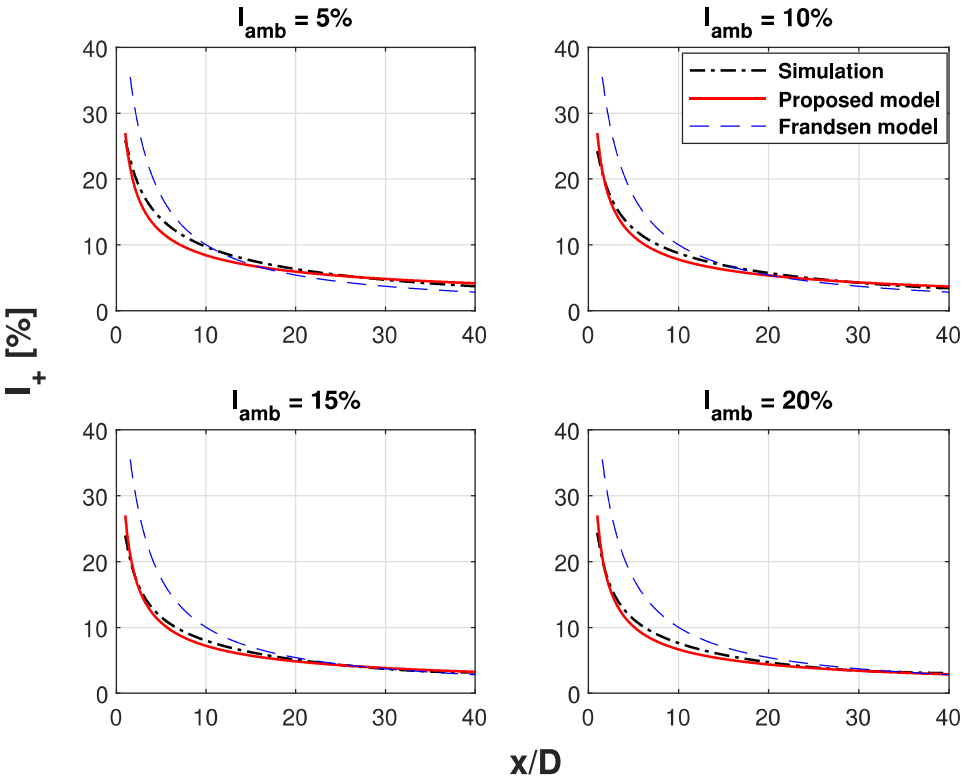

Figure 7: Comparison of centerline added turbulent intensity model with numerical simulation at different turbulent intensities.

Table 1: Mean absolute relative error of the added turbulent wake model.

Ambient turbulence	5%	10%	15%	20%
Proposed model	8.09	6.42	5.59	6.31

5 Conclusion

In this study, a series of numerical simulations of a 20 m diameter tidal turbine using the actuator disc method is carried out at different turbulent intensities. A simple empirical model for center-line added turbulent intensity is developed and compared with the existing Frandsen model. The empirical model justifies that the major turbulence source in the near wake is attributed to the rotor and the added turbulence is slightly dependent on the ambient turbulence in the flow. This model developed applies to realistic tidal stream conditions with a rotor operating at optimal thrust coefficient (Betz limit). This

study provides a foundation to develop a generalized model. The next step towards a generalized model is developing a model for multiple turbines in a park.

References

Abolghasemi, M. A., Piggott, M. D., Spinneken, J., Viré, A., Cotter, C. J., & Crammond, S. (2016). Simulating tidal turbines with multi-scale mesh optimisation techniques. *Journal of Fluids and Structures*, *66*, 69–90.

Chamorro, L. P., & Porté-Agel, F. (2009). A wind-tunnel investigation of wind-turbine wakes: boundary-layer turbulence effects. *Boundary-layer meteorology*, *132*(1), 129–149.

Crespo, A., Herna, J., et al. (1996). Turbulence characteristics in wind-turbine wakes. *Journal of wind engineering and industrial aerodynamics*, *61*(1), 71–85.

El Kasmi, A., & Masson, C. (2008). An extended k–ε model for turbulent flow through horizontal-axis wind turbines. *Journal of Wind Engineering and Industrial Aerodynamics*, *96*(1), 103–122.

Frandsen, S., & Thøgersen, M. L. (1999). Integrated fatigue loading for wind turbines in wind farms by combining ambient turbulence and wakes. *Wind Engineering*, 327–339.

Gant, S., & Stallard, T. (2008). Modelling a tidal turbine in unsteady flow. In *Proceedings of the eighteenth (2008) international offshore and polar engineering conference* (pp. 473–479).

Goss, Z., & Coles, D. (2020). Identifying economically viable tidal sites within the alderney race through optimization of levelized cost of energy. *Philosophical Transactions of the Royal Society A*, *378*(2178), 20190500.

Grondeau, M., Guillou, S. S., Poirier, J. C., Mercier, P., Poizot, E., & Méar, Y. (2022). Studying the wake of a tidal turbine with an ibm-lbm approach using realistic inflow conditions. *Energies*, *15*(6), 2092.

Harrison, M., Batten, W., Myers, L., & Bahaj, A. (2010). Comparison between cfd simulations and experiments for predicting the far wake of horizontal axis tidal turbines. *IET Renewable Power Generation*, *4*(6), 613–627.

IEC, S. (2019). *IEC 61400–1,Wind energy generation systems* (1.0 2019-04 ed.). IEC.

Jump, E., Macleod, A., & Wills, T. (2020). Review of tidal turbine wake modelling methods. *International Marine Energy Journal*, *3*(2), 91–100.

Mullings, H., & Stallard, T. (2021). Assessment of dependency of unsteady onset flow and resultant tidal turbine fatigue loads on measurement position at a tidal site. *Energies*, *14*(17), 5470.

Mycek, P., Gaurier, B., Germain, G., Pinon, G., & Rivoalen, E. (2014). Experimental study of the turbulence intensity effects on marine current turbines behaviour. part i: One single turbine. *Renewable Energy*, *66*, 729–746.

Nguyen, V. T., Guillou, S., Thiébot, J., & Santa Cruz, A. (2016). Modelling turbulence with an actuator disk representing a tidal turbine. *Renewable Energy*, *97*, 625–635.

Nguyen, V. T., Santa Cruz, A., Guillou, S. S., Shiekh Elsouk, M. N., Thiebot, J., et al. (2019). Effects of the current direction on the energy production of a tidal farm: the case of raz blanchard (france). *Energies*, *12*(13), 2478.

Olson, S. S., Su, J. C., et al. (2021). Turbulence-parameter estimation for current-energy converters using surrogate model optimization. *Renewable Energy*, *168*, 559–567.

Qian, G.-W., & Ishihara, T. (2021). Wind farm power maximization through wake steering with a new multiple wake model for prediction of turbulence intensity. *Energy*, *220*, 119680.

Quarton, D., & Ainslie, J. (1990). Turbulence in wind turbine wakes. *Wind Engineering*, 15–23.

Rajgor, G. (2016). Tidal developments power forward. *Renewable Energy Focus*, *17*(4), 147–149.

Réthoré, P.-E., Sørensen, N. N., Bechmann, A., & Zahle, F. (2009). Study of the atmospheric wake turbulence of a cfd actuator disc model. In *2009 european wind energy conference and exhibition* (pp. 1–9).

Roc, T., Conley, D. C., & Greaves, D. (2013). Methodology for tidal turbine representation in ocean circulation model. *Renewable Energy*, *51*, 448–464.

Shives, M., & Crawford, C. (2016). Adapted two-equation turbulence closures for actuator disk rans simulations of wind & tidal turbine wakes. *Renewable Energy*, *92*, 273–292.

Stallard, T., Feng, T., & Stansby, P. (2015). Experimental study of the mean wake of a tidal stream rotor in a shallow turbulent flow. *Journal of Fluids and Structures*, *54*. doi: 10.1016/j.jfluidstructs.2014.10.017

Taylor, G. I. (1958). *The scientific papers of sir geoffrey ingram taylor: Mechanics of solids* (Vol. 1). CUP Archive.

Thiébaut, M., Filipot, J.-F., Maisondieu, C., Damblans, G., Jochum, C., Kilcher, L. F., & Guillou, S. (2020). Characterization of the vertical evolution of the three-dimensional turbulence for fatigue design of tidal turbines. *Philosophical Transactions of the Royal Society A*, *378*(2178), 20190495.

Vermeer, L., Sørensen, J. N., & Crespo, A. (2003). Wind turbine wake aerodynamics. *Progress in aerospace sciences*, *39*(6-7), 467–510.

Zhang, Y., Fernandez-Rodriguez, E., Zheng, J., Zheng, Y., Zhang, J., Gu, H., … Lin, X. (2020). A review on numerical development of tidal stream turbine performance and wake prediction. *IEEE Access*, *8*, 79325–79337.